THE STRUCTURAL DESIGN OF TALL AND SPECIAL BUILDINGS
Struct. Design Tall Spec. Build. **22**, 1199–1214 (2013)
Published online 8 February 2012 in Wiley Online Library (wileyonlinelibrary.com/journal/tal). DOI: 10.1002/tal.762

Progressive collapse behavior of rotor-type diagrid buildings

Jinkoo Kim*,† and Jieun Kong

Department of Architectural Engineering, Sungkyunkwan University, Suwon, Korea

SUMMARY

In this study, the progressive collapse-resisting capacities of axi-symmetric or rotor-type diagrid structural system buildings were evaluated based on arbitrary column removal scenario. For analysis models, 33-story buildings with cylindrical, convex, concave and gourd shapes were designed, and their nonlinear static and dynamic analysis results were compared. The effect of design variables such as the number of total stories, slope of diagrids and the location of removed members was also investigated. According to the analysis results, the rotor-type diagrid structures showed sufficient progressive collapse-resisting capacity regardless of the differences in shapes when a couple of diagrids were removed from the first story. The design parameter such as building height and the slope of the diagrids did not affect the results significantly as long as they were designed to meet the current design code. Copyright © 2012 John Wiley & Sons, Ltd.

Received 21 October 2011; Accepted 9 December 2011

KEYWORDS: progressive collapse; diagrid; nonlinear analysis; tall buildings

1. INTRODUCTION

Current trends in the design of tall buildings are driven by diverse factors such as the demand for taller height, the need for improved safety against fire and terrorist attacks and the characteristic forms that can provide distinct identity for the buildings. These requirements have led to new solutions for structural systems and form-generation techniques. Park *et al.* (2004) discussed a parametric design process for form generation of tall buildings based on the architectural and structural criteria. Vollers (2008) proposed a morphological scheme that enables data to be retrieved on sustainable performance of building shapes. He categorized the geometry of high-rise buildings into *extruders*, *rotors*, *twisters*, *tordos*, *transformers* and *free shapers* depending on their form-generation method. Among the high-rise building forms, *rotor* is a building volume created by rotating a line around a vertical axis. When the line is vertical, the volume is a cylinder. When the line is inclined, a hyperboloid results. The Tornado Tower in Doha, Qatar, is an example of a recently built hyperboloid-shaped building. A semicircle with its ends on the rotation axis when rotated results in a globe. Rotational building models can be made to bulge (a *bulging rotor*) or squeeze (a *squeezed rotor*) just by manipulating the curve that is rotated.

Recently, diagrid systems are emerging as structurally efficient as well as architecturally pleasing structural systems for tall buildings. The diagrid system has been applied for structural design of axi-symmetric structures such as the Swiss-Re building in London and the Tornado Tower. The diagonal members in diagrid structural systems can carry gravity loads as well as lateral forces due to their triangulated configuration in a distributive and uniform manner. Compared with conventional framed tubular structures without diagonals, diagrid structures are more effective in minimizing shear deformation because they carry shear by axial action of the diagonal members, while conventional tubular structures carry shear by the bending of the vertical columns and horizontal spandrels (Moon, 2007). Kim and Lee (2010) showed that the tube-type diagrid structure generally had high progressive collapse-resisting capacity.

*Correspondence to: Jinkoo Kim, Department of Architectural Engineering, Sungkyunkwan University, 300 Cheoncheon-dong, Jangan-gu, Suwon, 440-746, Korea.
†E-mail: jkim12@skku.edu

The current trend of minimizing the number of interior and exterior columns to provide wide open interior space and outside view results in enhanced progressive collapse potential in modern tall buildings. Shi *et al.* (2010) reviewed current progressive collapse analysis methods available in the literature, discussed their suitability, applicability and reliability and proposed a new method for progressive collapse analysis of reinforced concrete frames under blast loads. Kim and Hong (2011) investigated the progressive collapse-resisting capacities of tilted or twisted buildings and compared their performances with those of regular buildings. They found that the progressive collapse potential of the tilted structures varied significantly depending on the location of the removed column and that the progressive collapse potential of the twisted structures is not reduced significantly since they were designed with more structural steel to satisfy design loads and more structural elements are involved in resisting progressive collapse when a structural member is eliminated.

In this study, among the various forms of tall buildings stated above, the *rotor*-type buildings with different vertical curvatures were designed using diagrid systems, and their collapse behaviors were evaluated based on arbitrary column removal scenario. For analysis models, 33-story buildings with cylindrical, convex, concave and gourd-type elevations and circular plan shape were designed, and their performances were compared. The effect of design variables such as the number of total stories, slope of diagrids and the location of removed members was also investigated.

2. DESIGN AND ANALYSIS MODELING OF CASE STUDY STRUCTURES

The analysis model structures are 33-story structures with the cylindrical, lower and upper convex, concave and gourd shapes as shown in Figure 1. The structures with cylindrical shape were designed as both moment frame (Figure 1(a)) and diagrid (Figure 1(b)), and the other structures were designed with diagrid system. Figure 2 depicts the structural plan shape of the cylinder-type structure. To compare their performances at equal basis, the model structures were designed to have similar overall floor areas for the same design loads. The perimeter beams and columns were designed with H-shaped rolled sections, and the diagrid members were designed with circular hollow steel sections. The floor slabs were considered as rigid diaphragm. The model structures were designed with dead and live loads of 6 and 2.5 kN/m^2, respectively, and wind load with basic wind speed of 30 m/s. The seismic load was evaluated based on the spectral acceleration coefficients of $S_{DS} = 0.43$ and $S_{D1} = 0.23$ with the response modification factor of 3.0 in the ASCE 7-10 (2010) format. The structural design was carried out using the structural analysis/design program code MIDAS (MIDAS IT, Seoul, Korea, 2007) based on the AISC LRFD Specifications (AISC 2000). Then, the design information was exported to the SAP 2000 (Computers and Structures, Berkeley, CA, USA, 2004) to evaluate the progressive collapse-resisting capacity of the model structures. In most cases, the core was designed to resist only gravity load, and the perimeter frame or diagrid system was designed to resist all the lateral loads. Only the cylinder-type structure with exterior moment-resisting frame (MRF) was designed in two different ways. In the first case, the exterior moment frame was designed to resist all the lateral loads (lateral load-resisting systems, LLRS) as in the other analysis models, and in the second case, the exterior moment frame was designed to resist only gravity load, and the lateral loads were resisted by a braced core (gravity load-resisting system, GLRS). Table 1 shows the total floor areas and the steel tonnage of the perimeter structures. It can be observed that the cylinder-type LLRS structure was designed with structural steel 1.6 times larger than that of the GLRS structure, which was designed with similar steel tonnage to that of the other diagrid structures. On the basis of these results, it was concluded that the diagrid is a more efficient load-resisting system than the moment frame is. It can also be observed that the upper-convex type structure with higher mass center and the gourd-type structure with rapid variation in curvature were designed with larger steel tonnage.

For nonlinear analysis of bending members, the skeleton curve provided in the FEMA-356 (2000) and shown in Figure 3(a) was used. The parameters *a*, *b*, and *c* vary depending on the width–thickness ratio of the structural members and were determined based on the guidelines provided in the Tables 5-6 and 5-7 of the FEMA-356. The post-yield stiffness of 3% was generally used for modeling of bending members. For nonlinear analysis of truss and bracing members, the generalized load–deformation curves recommended in the FEMA-274 (1997) and shown in Figure 3(b) were used. Figure 3(a) also

DOI: 10.1002/tal

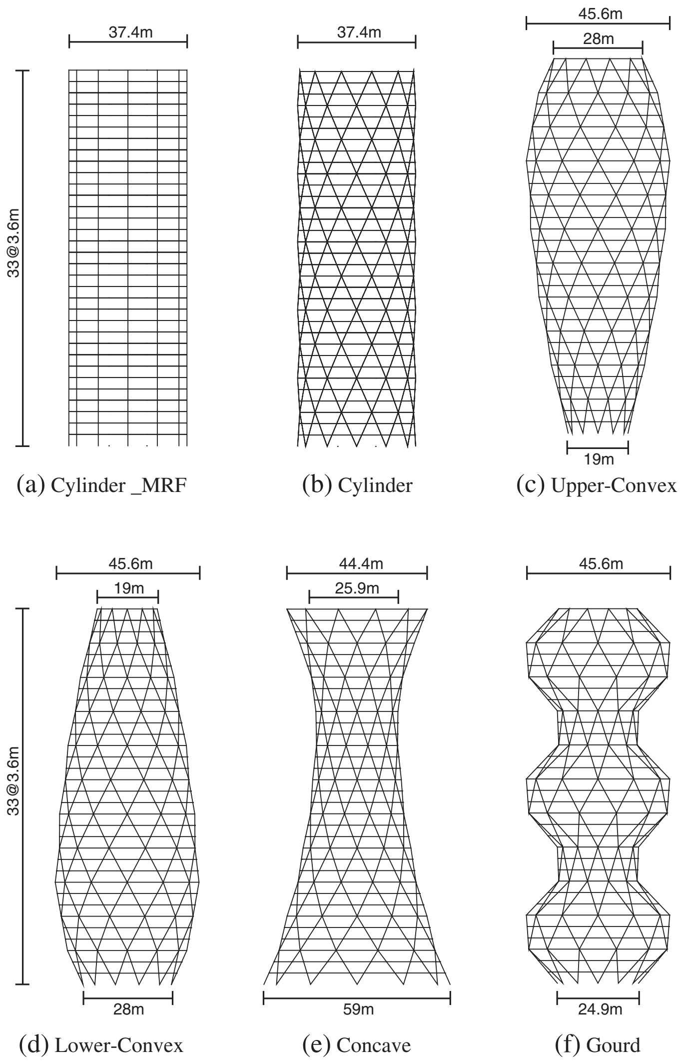

Figure 1. Elevation of 33-story buildings with shape.

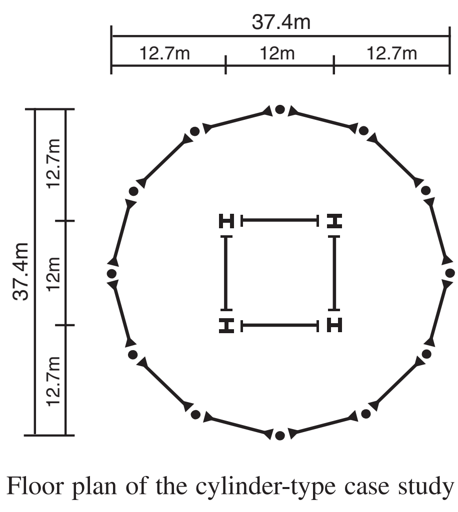

Figure 2. Floor plan of the cylinder-type case study buildings.

DOI: 10.1002/tal

Table 1. Floor area of analysis model structures and steel tonnage of their exterior structures.

Type	Floor area (m^2)	Weight of perimeter structure (tonf)
Cylinder (diagrid)	34 981	949
Cylinder (MRF_LLRS)	34 619	1592
Cylinder (MRF_GLRS)	34 619	838
Upper convex	34 965	1172
Lower convex	35 325	1015
Concave	35 308	1070
Gourd	35 120	1253

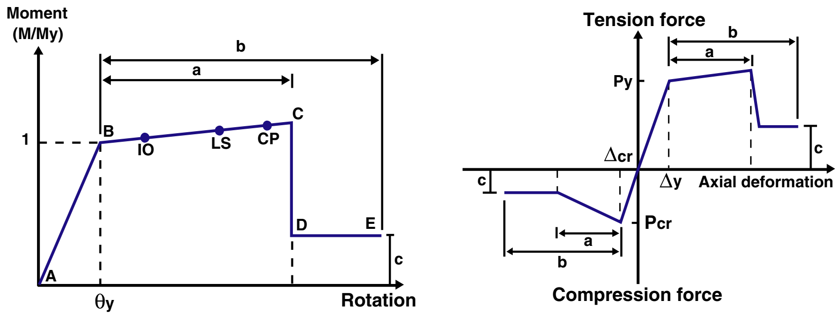

(a) Flexural members (b) Braces

Figure 3. Nonlinear force–deformation relationships for structural members.

shows the deformation levels corresponding to the immediate occupancy (IO), life safety (LS) and collapse prevention (CP) performance points as specified in the FEMA-356.

3. PERFORMANCE OF CYLINDER-TYPE STRUCTURES

3.1. Nonlinear static and dynamic analysis procedures

The progressive collapse performance of the analysis model structures was investigated based on the arbitrary column-loss scenario. The finite element program code SAP 2000 (2004) was used for nonlinear static and dynamic analysis. For static analysis of moment frames, the General Services Administration (GSA) guidelines recommend the dynamic amplification factor of 2.0 in the applied load to account for dynamic redistribution of forces. The load combination of GSA (2003) for static analysis is 2(Dead Load + 0.25 × Live Load).The pushdown analysis is generally applied not to determine whether the structure will fail or not but to evaluate the residual strength of the structure after a column is removed. In this study, pushdown analyses of the model structure were carried out by removing one of the first-story columns in the cylinder-type moment frame structure or a pair of diagrid bracing in the other structures. The displacement-controlled pushdown analysis was carried out by increasing 1 mm at a time the vertical displacement of the joint from which the column/diagrids removed and computing the corresponding load.

In the dynamic analysis, no amplification factor was applied to the imposed gravity load. In order to carry out dynamic analysis, the member forces of a column, which is to be removed to initiate progressive collapse, are computed before it is removed. Then, the column is replaced by the point loads equivalent of its member forces. To simulate the phenomenon that the column is removed by impact or blast, the column member forces are suddenly removed after elapse of a certain time while the gravity load remains unchanged as shown in Figure 4. In this study, the member reaction forces are increased linearly for 10 s until they reach the specified level, are kept unchanged for 5 s until the system reaches stable condition and are suddenly removed at 15 s to initiate progressive collapse. The damping ratio was assumed to be 5% of the critical damping. The diagrid structure had an intermediate value of 1.24.

DOI: 10.1002/tal

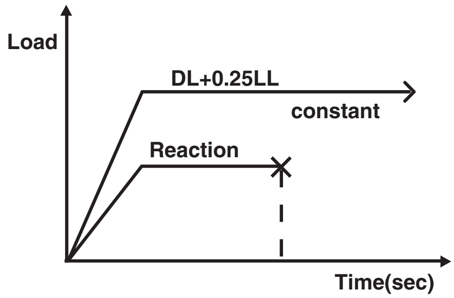

Figure 4. Time histories of imposed loads for dynamic analysis.

As mentioned earlier, dynamic amplification factor is required in the nonlinear static analysis. The amplification factor of 2.0 recommended in the GSA guidelines may be appropriate for MRFs with vertical rectangular grid of beams and columns. However, in the diagrid structure, in which there exist numerous vertical load paths when a pair of diagrids is removed, the dynamic amplification of member forces may be different. Figure 5(a and 5(b) show the member force ratios of the cylinder-type diagrid structure obtained from dynamic and static analyses after removing one and two pairs of diagrids from the first story, respectively. The perimeter diagrid structure was designed to resist both gravity and lateral loads with 65.9° diagrid slope. It can be observed that in a few diagrid members located in the lower few stories and in the top story, the ratio exceeded 1.5. However, in most members, the dynamic amplification is less than 50%. It can also be noticed that compared with the case of moment frames, in which the dynamic amplification is mostly limited to the members located right above the lost column, wider range of members was affected by the dynamic effect. In this study, with the analysis results, the dynamic amplification factor of 1.5 was applied uniformly in all floor areas for static analysis to compute the failure load in the conservative side.

Figure 6 shows the nonlinear static and dynamic analysis results of the cylinder-type MRF designed for resisting both gravity and lateral load (MRF_LLRS), the moment frame designed only for gravity load (MRF_GLRS) and the diagrid structure with 65.9° diagrid angle. To initiate progressive collapse, a

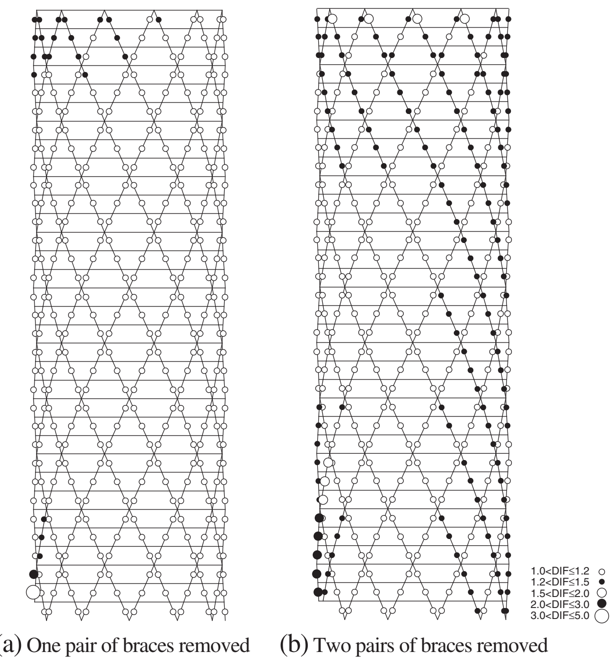

Figure 5. Ratio of member forces obtained from dynamic and static analysis.

DOI: 10.1002/tal

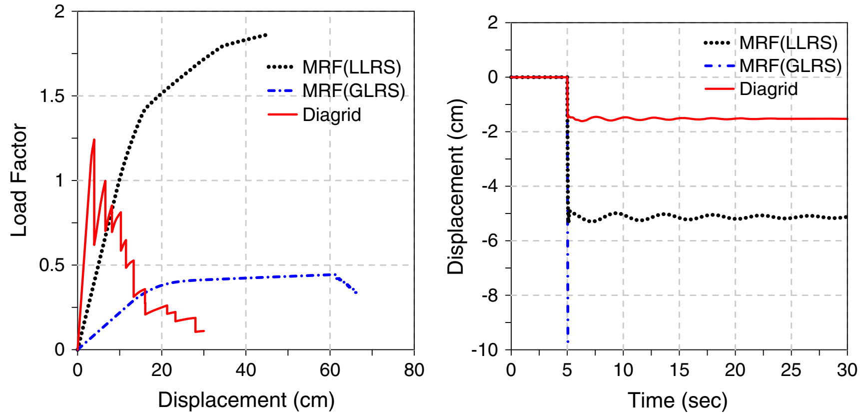

(a) Nonlinear static analysis (b) Nonlinear dynamic analysis

Figure 6. Analysis results of regular structures.

column (MRF) or a pair of diagrids was removed from the first story, and the force–vertical displacement relationship was plotted in Figure 6(a). The vertical axis represents the load factor, which is the applied load divided by the GSA specified load combination. It can be observed that the LLRS moment frame showed the highest maximum load factor of 1.86 and the GLRS showed the lowest value of 0.34. The maximum load factor of the diagrid structure turned out to be the intermediate value of 1.24. The LLRS moment frame and the diagrid structure, which showed the maximum load factor of 1.0, may be considered safe against progressive collapse triggered by the loss of a first-story column or a pair of diagrids. However, the GLRS moment frame with the maximum load factor significantly less than 1.0 is prone to fail as a result of column loss. This can be confirmed by the nonlinear dynamic analysis results presented in Figure 6(b). The figure shows that the vertical displacement of the GLRS structure increased unbounded right after a first-story column was suddenly removed. It can be observed that the other two structures remained stable. The vertical displacement of the diagrid structure was smaller than that of the LLRS MRF.

Figure 7 shows the plastic hinge formation of the three cylinder-type model structures at their maximum strengths. In the LLRS structure, plastic hinges formed at beam ends in nine stories above the lost column. The analysis stopped when plastic hinges finally formed at the second-story columns. In the GLRS structure, plastic hinges formed in all beams located at the bays from which the column

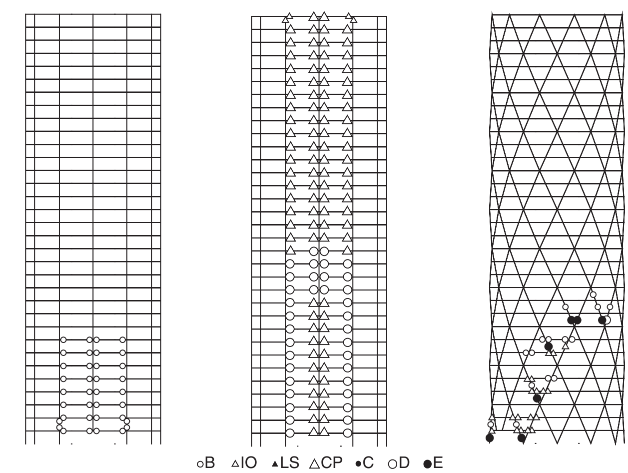

(a) LLRS (b) GLRS (c) Diagrid

Figure 7. Plastic hinge formation in the cylinder-type models.

DOI: 10.1002/tal

was removed. When a pair of diagrids was removed from the first story, yielded or buckled members propagated diagonally up to the 11th story before the analysis was stopped.

Figure 8 depicts the pushdown curves of the cylinder-type diagrid structures with the slope of diagrid varying from 36.6° to 83°. The steel tonnage for each model structure is shown in Table 2, where it can be observed that the structure designed with smallest diagrid angle (36.6°) required the largest amount of structural steel, and the structure with 75° diagrid was designed with the smallest steel. The results correspond well with the research of Moon *et al*. (2007). The structure having 36.6° diagrid was designed with the largest structural steel; however, the maximum load factor turned out to be similar to the other structures. The structure with 83° diagrid, which was designed with 14% larger structural steel than the structure with 75° diagrid, showed the largest maximum load factor of 1.5 but the smallest stiffness. Figure 9 depicts the plastic hinge formation of the model structures near failure point. Starting from the second story, plastic hinges formed following the slope of the diagrid. In the structure having 36.6° diagrid, plastic hinges formed concentrated in the lower few stories and stopped in the fourth story, whereas in the structure with 75° and 83° diagrid, plastic hinges formed distributed throughout the stories.

To investigate the progressive collapse-resisting capacity of cylinder-type diagrid structures depending on their number of stories, structures with 65.9° diagrid were designed to have nine to 45 stories in the interval of six stories. Pushdown analyses were carried out removing a pair of diagrids from the first story. According to the pushdown curves shown in Figure 10, the maximum load factors of the model structures up to 33 stories reached about 1.2, and no difference in maximum strength was observed depending on the number of stories. In the structures with 39 and 45 stories, the maximum strength increased slightly as the number of story increased and reached up to 1.6 in the 45-story structure. The plastic hinge formations of the model structures are presented in Figure 11. It can be observed that in the structures with up to 21 stories, the plastic hinges (and the buckled members) propagated throughout the stories up to the top, whereas in the taller structures, the vertical propagation of plastic hinges stopped in a certain story and then continued horizontally until failure state was reached.

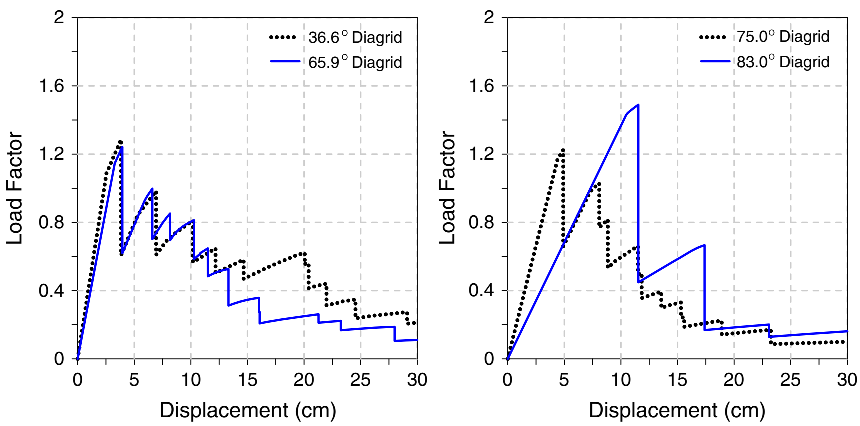

Figure 8. Nonlinear analysis results of cylinder-type models with various diagrid angles.

Table 2. Steel tonnage of perimeter structures of the cylinder-type buildings depending on the slope of the diagrid.

Slope (°)	Weight of perimeter structure (tonf)
36.6	1666
65.9	949
75.0	943
83.0	1077

DOI: 10.1002/tal

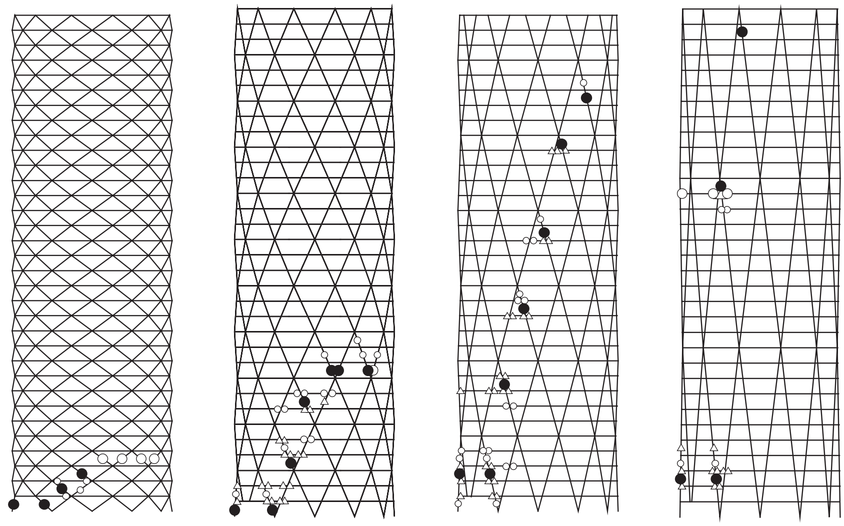

Figure 9. Plastic hinge formation of cylinder-type models with various diagrid angles.

Figure 12 shows the pushdown curves of the 33-story cylinder-type structure with 65.9° diagrid subjected to loss of a pair of diagrids at different stories. The amplified gravity load was applied on the levels above the story from which the members were removed. It can be observed that as the location of the removed members increased in height, the stiffness and strength generally decreased slightly except the case in which a pair of diagrids was removed from the 31st story. Figure 13 depicts the plastic hinge formation characteristics of the model structures depending on the locations of the member removal. As in the case of member removal from the first story, plastic hinges propagated along the slanted diagrids directly above the removed members. The overall patterns for plastic hinge formation turned out to be quite similar to those obtained by removing diagrids at the first story.

Figure 14 presents the analysis results of the cylinder-type structure with 65.9° diagrid subjected to loss of two pairs of diagrids in the first story. The force–displacement relationship obtained from pushdown analysis is shown in Figure 14(a), where it can be observed that the maximum load factor is 0.81, which is a 34% reduction compared with the case of removing a single pair of diagrids depicted in Figure 6(a). Figure 14(b) shows the time history of the vertical displacement obtained from nonlinear time history analysis. Due to the removal of one more pair of diagrids, the vertical displacement increased from 1.5 cm to 4.5 cm; nonetheless, the structure remained stable even after two pairs of diagrids were suddenly

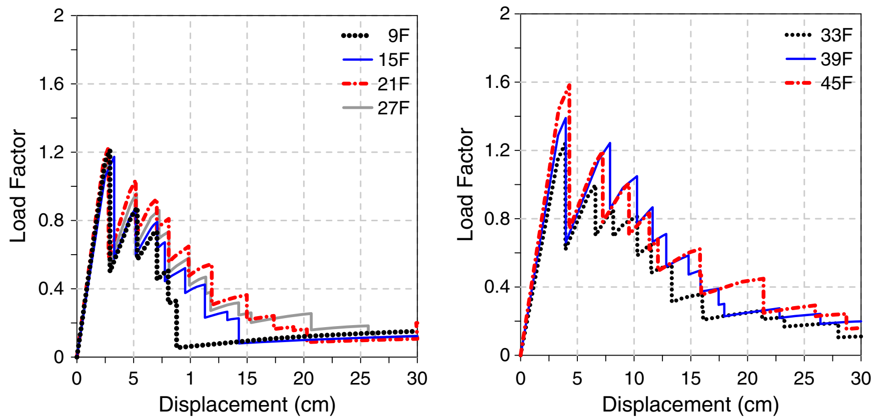

Figure 10. Nonlinear analysis results of cylinder-type structures with various number of stories.

DOI: 10.1002/tal

removed. Figure 14(c) depicts the plastic hinge formation of the structure, where it can be observed that the plastic hinge propagation pattern is similar to that of the structure with a pair of diagrids removed.

4. PERFORMANCE OF OTHER ROTOR-TYPE STRUCTURES

Figure 15(a) depicts the pushdown curves of the axi-symmetric structures shown in Figure 1(c–f) subjected to loss of a pair of first-story diagrid bracing. The pushdown curve for upper-convex model shown in Figure 1(c) kept increasing until the vertical displacement reached 3 cm and the load factor reached 1.6, and the analysis stopped when the diagrids at the 23rd and 24th stories buckled. As the

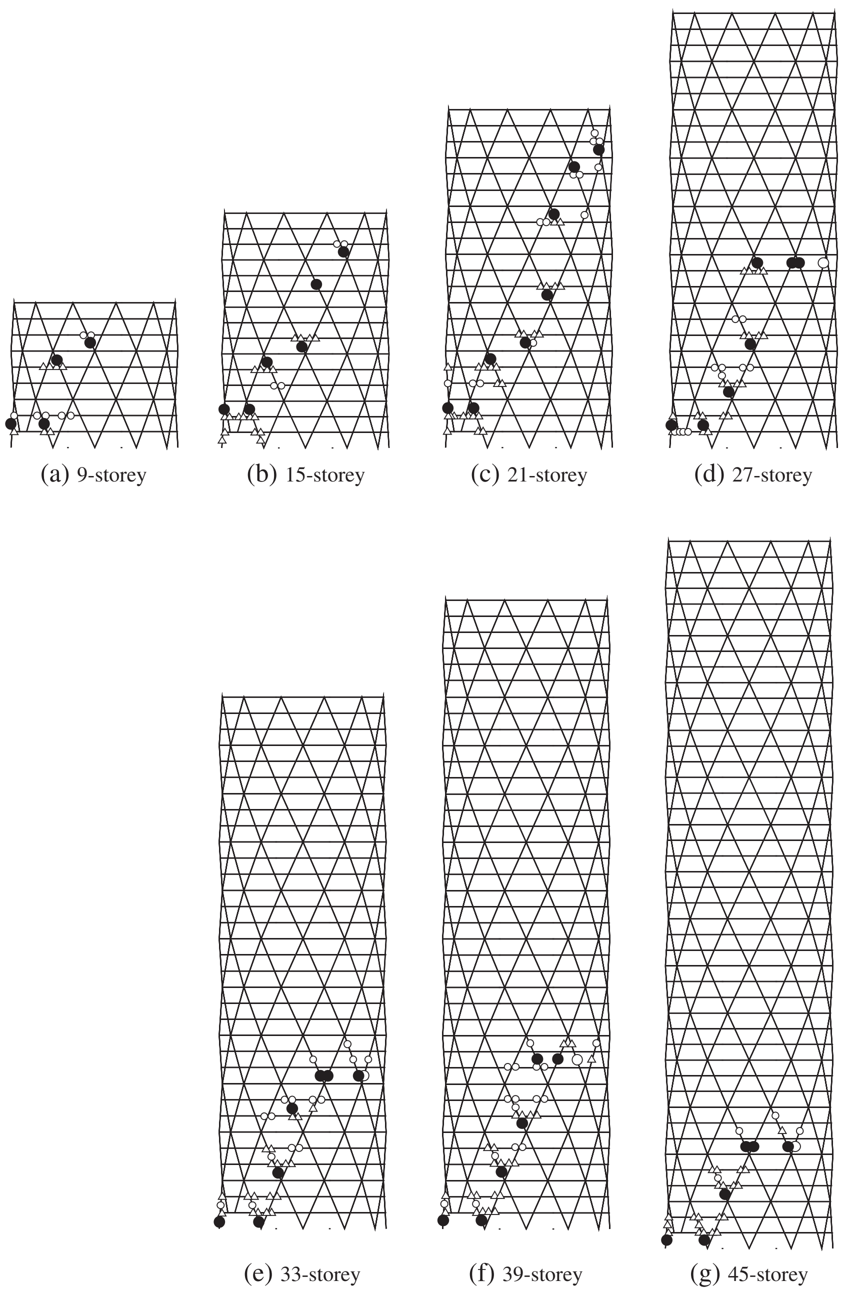

(a) 9-storey (b) 15-storey (c) 21-storey (d) 27-storey

(e) 33-storey (f) 39-storey (g) 45-storey

Figure 11. Plastic hinge formation in cylinder-type structures with various number of stories.

DOI: 10.1002/tal

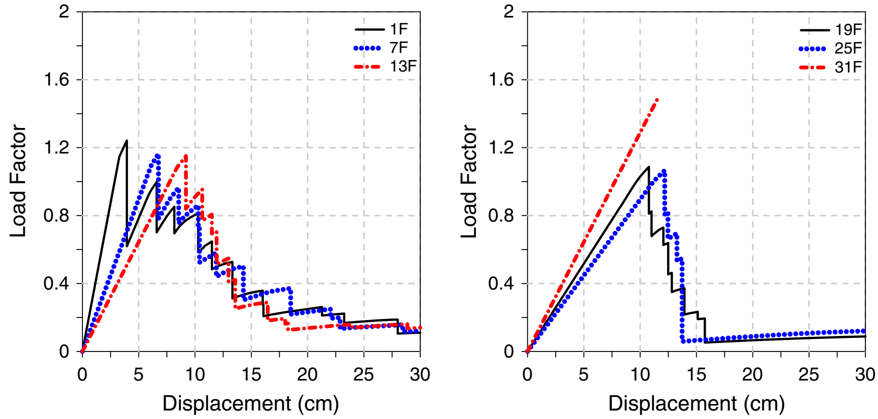

Figure 12. Pushdown curves of the 33-story cylinder-type structure depending on the location of the diagrid removed.

maximum load factor turned out to be higher than 1.0, the structure is considered to have enough strength against progressive collapse triggered by the removal of a pair of diagrids from the first story. The pushdown curve of the lower-convex model structure with relatively low mass center showed slightly smaller stiffness and strength, but the analysis continued until full descending branch was obtained. The maximum load factor of the gourd-type structure reached 1.5 and is considered to have enough strength against progressive collapse. The maximum load factor of the concave-type structure, which is also known as a hyperboloid, reached the smallest load factor of 0.97 with similar stiffness to the gourd-type structure. Figure 15(b) shows the vertical displacement time histories of the model structures, where it can be observed that all model structures remained stable after sudden removal of a pair of diagrids. The upper-convex model structure showed the smallest vertical displacement of about 1.2 cm, and the maximum displacement of the lower-convex structure is 1.5. The concave and the gourd-type structures showed the maximum vertical displacement of approximately 2.0 cm. Figure 16 depicts the formation of plastic hinges or buckled members of the four rotor-type structures when their maximum strengths were reached in the nonlinear static pushdown analysis. In the lower-convex and concave-type structures, plastic hinges propagated up to the 12th story when a pair of diagrids was removed from the first story. In the upper-convex structure, plastic hinges formed concentrated in the 16th, 20th and 24th stories. In those stories, plastic hinges spread horizontally. It was observed that at the vertical displacement of 3 cm, many plastic hinges formed in the 24th stories and the analysis was stopped. In the gourd-type structure with rapid variation of vertical curvature, the plastic hinges formed concentrated in the lower four stories. When the damaged members reached the fourth story, they propagated laterally until failure.

Figure 17(a) presents the force–displacement relationships of the rotor-type structures subjected to loss of two pairs of diagrids in the first story. It can be observed that the removal of one more pair of diagrids resulted in about 30% reduction in the maximum load factor. The maximum load factor of the concave model is the minimum value of 0.69. The maximum load factor of 1.37 was observed in the upper-convex model, which is reduced by 14% from the value obtained by removal of single pair of diagrids. The maximum strengths of the other structures also somewhat decreased compared with those obtained by removing only a pair of diagrids; however, in many cases, the maximum load factors still remained above 1.0, and the structures are considered to be safe against progressive collapse caused by the removal of two pairs of diagrids from the first story. The time-history analysis results depicted in Figure 18(b) shows that the vertical displacement of the concave-type structure with its maximum load factor well below 1.0 increased unbounded as soon as the two pairs of diagrids were suddenly removed, while the upper-convex, the lower-convex and the gourd-type structures remained stable even after the removal of two pairs of diagrids. The plastic hinge formation patterns shown in Figure 18 are similar to those obtained by removing a pair of diagrids.

DOI: 10.1002/tal

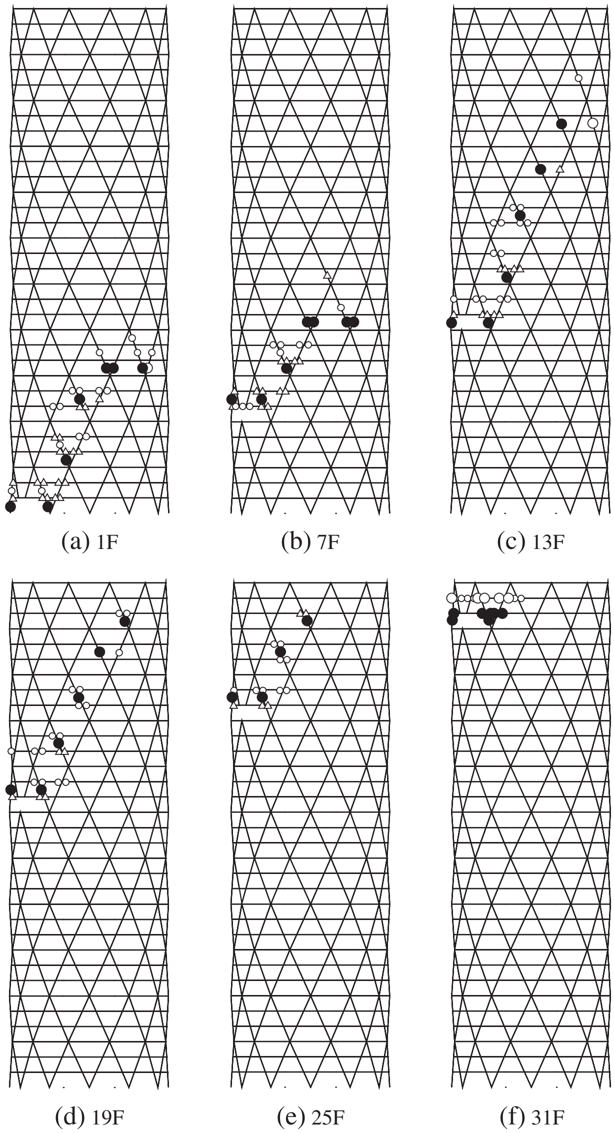

Figure 13. Plastic hinge formation in the cylinder-type models depending on the location of the diagrid removed.

Figure 19 shows the pushdown curves of the gourd-type structure subjected to loss of a pair of diagrids at different locations throughout the height. Similar to the results of the cylinder-type structure, the stiffness of the pushdown curve kept decreasing as the height of the column removal increased. The strength was largest when the members were removed from the first story and was the smallest when they were removed from the 16th story. The location of the damaged members are shown in Figure 20, where it can be observed that the plastic hinges or buckled members did not propagate vertically as observed in other types of structures but formed concentrated in each structural module. As a result of rapid change in vertical curvature, the plastic hinges generally spread horizontally rather than vertically.

5. CONCLUSIONS

In this study the progressive collapse-resisting capacities of rotor-type or axi-symmetric diagrid buildings were evaluated by nonlinear static and dynamic analyses. For analysis models, 33-story buildings with cylindrical, convex, concave and gourd-type elevations and circular plan shape were designed, and their

DOI: 10.1002/tal

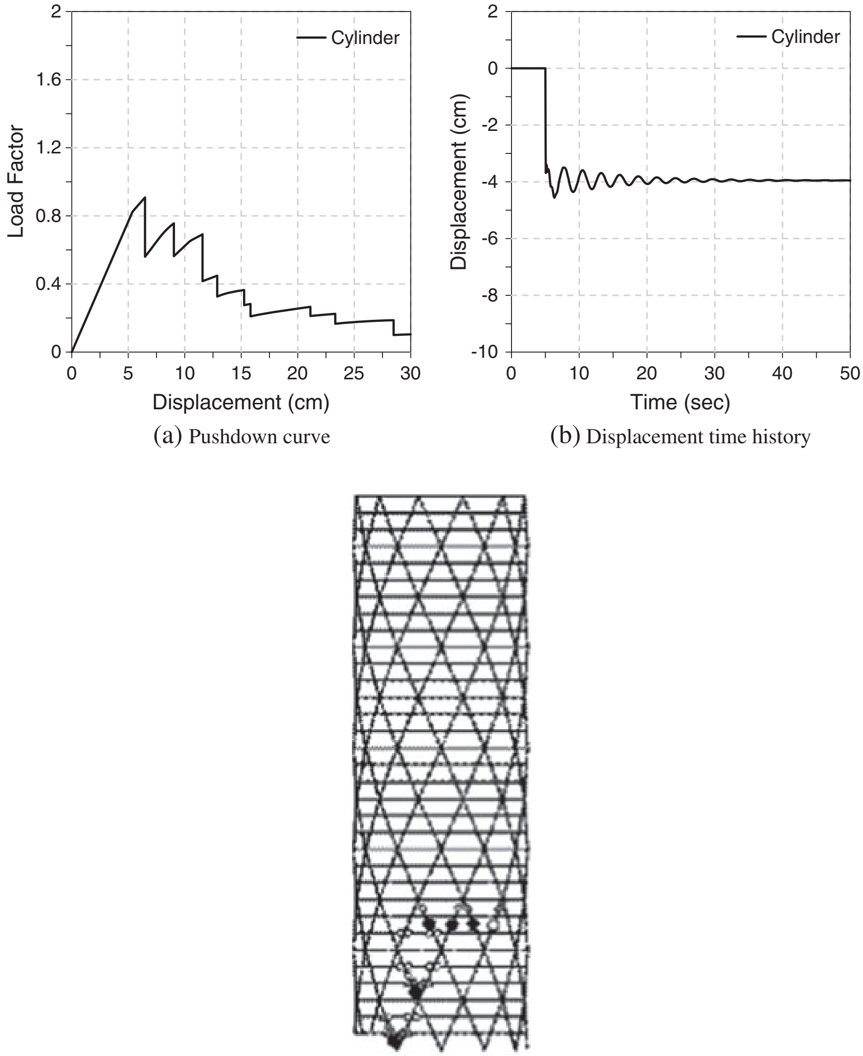

(a) Pushdown curve

(b) Displacement time history

(c) Plastic hinge formation

Figure 14. Analysis results of the cylinder-type diagrid structure subjected to loss of two pairs of diagrids.

performances were compared. The effect of design variables such as the number of stories, slope of diagrids and the location of removed members was also investigated.

According to the analysis results, the rotor-type diagrid structures showed sufficient progressive collapse-resisting capacity regardless of the differences in shapes when a column or a pair of diagrid bracing was removed from the first story except for the MRF designed only for gravity loads. However, when two pairs of diagrids were removed from the first story, progressive collapse occurred in the concave-type structure. In the cylinder-type structure with relatively small inclination angle of diagrids, the plastic hinges and buckled members formed in the lower stories; as the inclination angle of diagrids increased, they propagated farther to the top. The stiffness of the load–displacement relationship and the maximum strength generally decreased as the location of member removal increased in height. The damaged members in the gourd-type structure with large variation in vertical curvature did not spread widely but were concentrated in a few stories right above the location of the removed members. The design parameter such as building height and the slope of the diagrids did not affect the maximum strength significantly.

DOI: 10.1002/tal

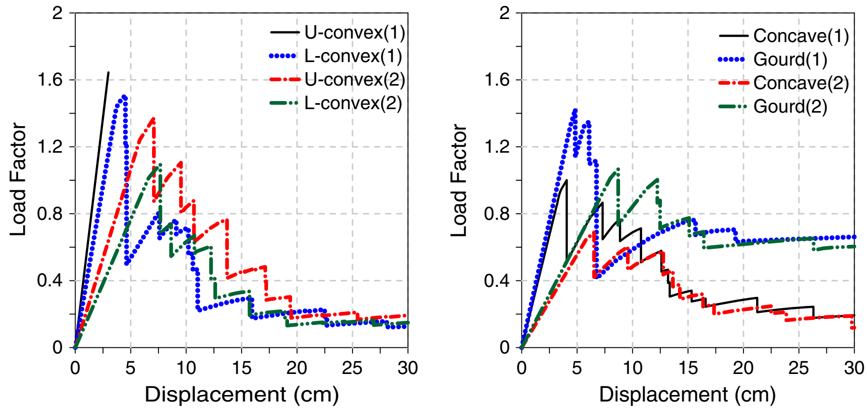

(a) Nonlinear static analysis

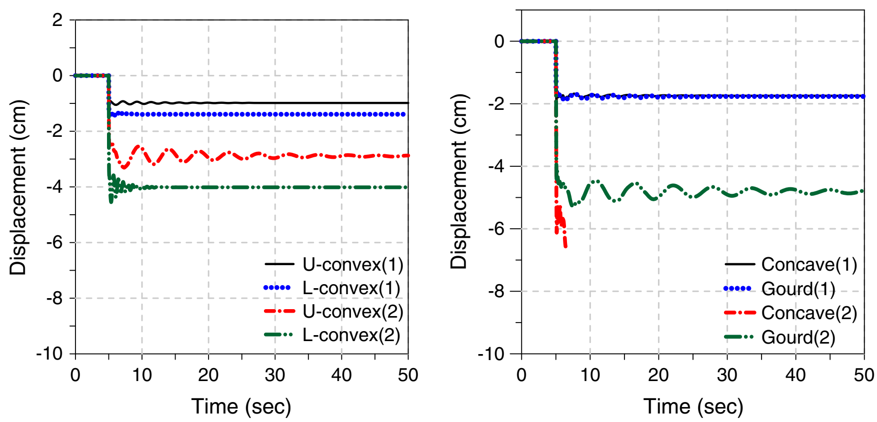

(b) Nonlinear dynamic analysis

Figure 15. Nonlinear analysis results of various axi-symmetric structures subjected to loss of a pair of diagrid in the first story.

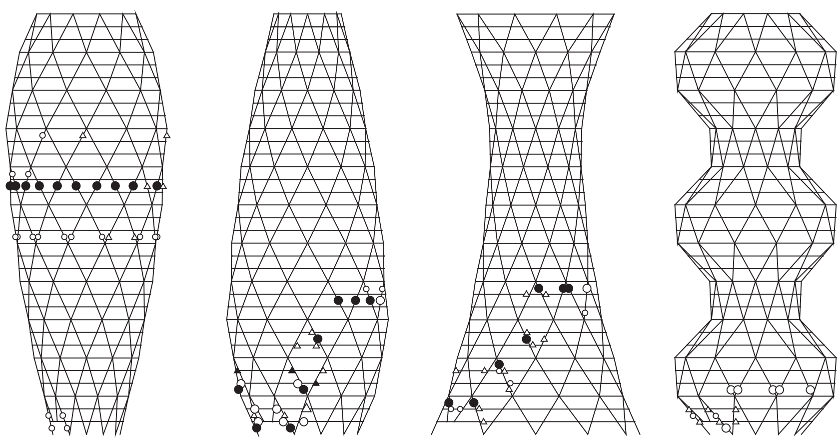

(a) Upper-Convex (b) Lower-Convex (c) Concave (d) Gourd

Figure 16. Plastic hinge formation in the various axi-symmetric structures subjected to loss of a pair of diagrids in the first story.

DOI: 10.1002/tal

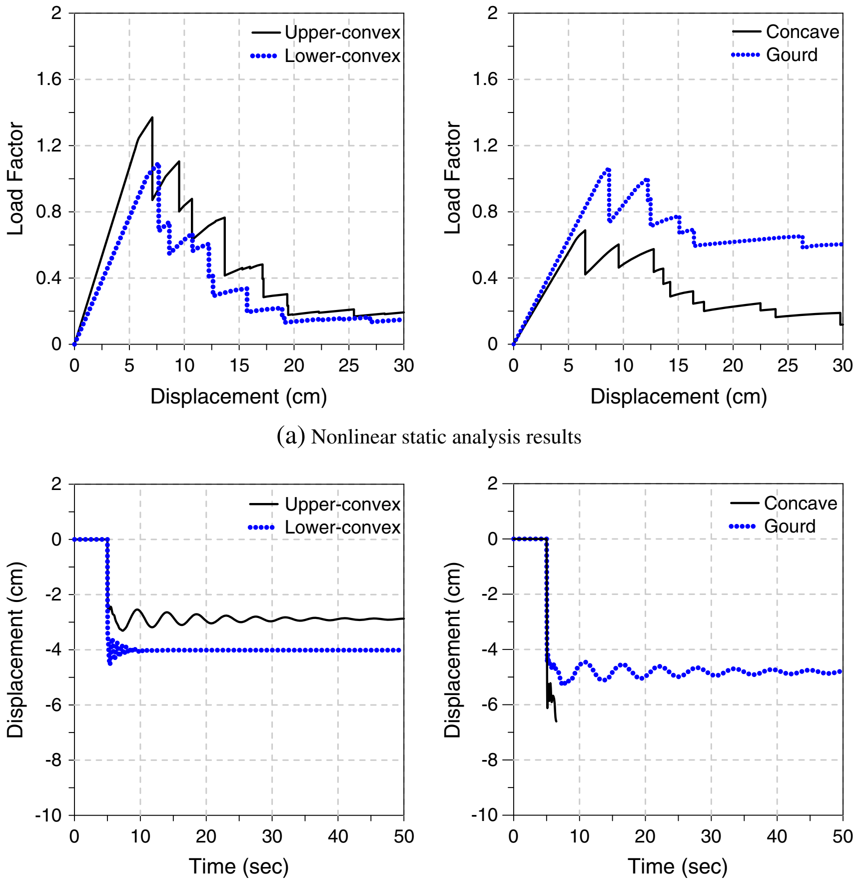

(a) Nonlinear static analysis results

(b) Nonlinear dynamic analysis results

Figure 17. Nonlinear analysis results of various axi-symmetric structures subjected to loss of two pairs of diagrids in the first story.

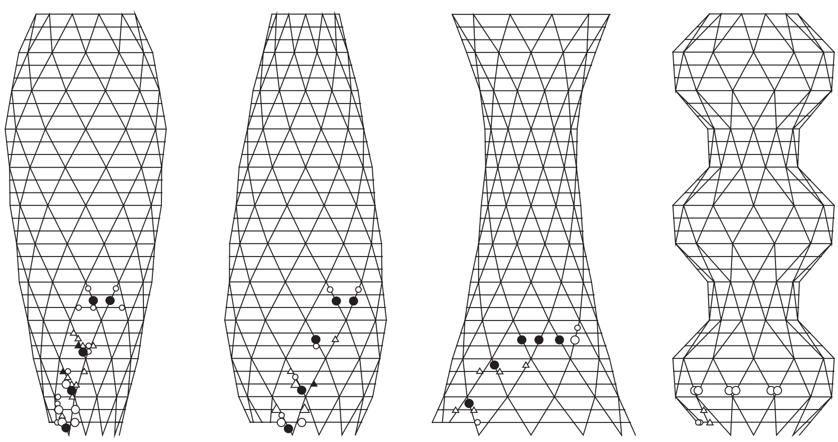

(a) Upper-Convex (b) Lower-Convex (c) Concave (d) Gourd

Figure 18. Plastic hinge formation in the various axi-symmetric structures subjected to loss of two pairs of diagrids in the first story.

DOI: 10.1002/tal

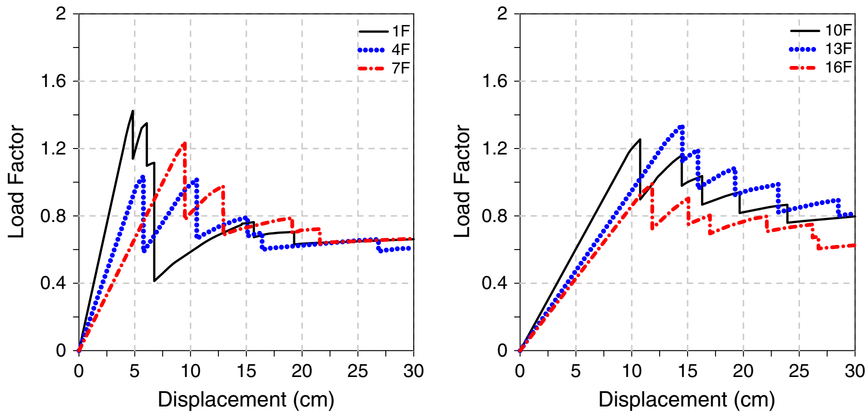

Figure 19. Nonlinear analysis results of gourd-type structure depending on the location of the diagrid removed.

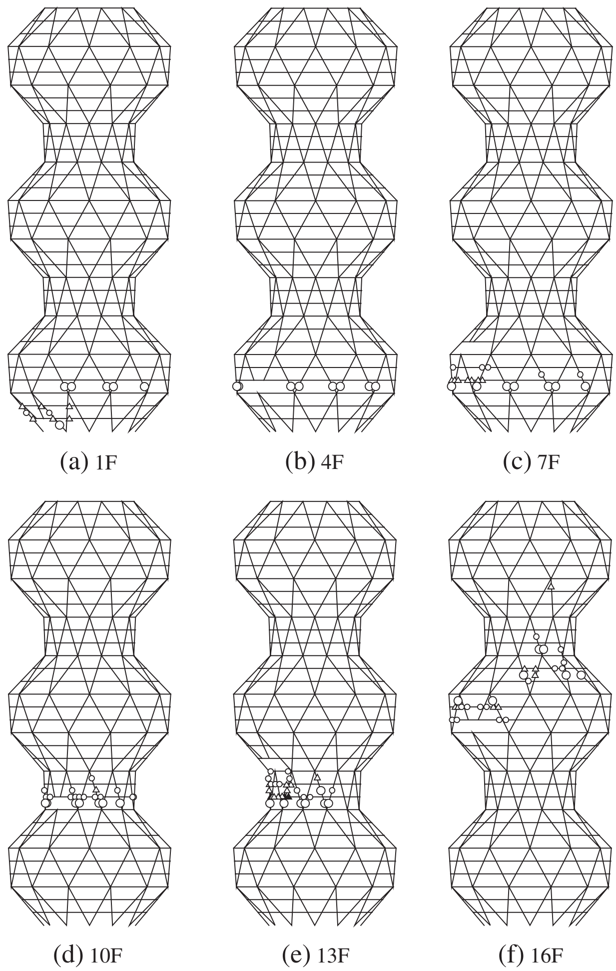

Figure 20. Plastic hinge formation of gourd-type structure depending on the location of the diagrid removed.

DOI: 10.1002/tal

ACKNOWLEDGEMENT

This research was supported by a grant (code # '09 R&D A01) funded by the Ministry of Land, Transport and Maritime Affairs of the Korean government.

REFERENCES

AISC. 2000. *Load and Resistance Factor Design Specification for Structural Steel Buildings*. American Institute of Steel Construction: Chicago.

ASCE 7-10. 2010. *Minimum Design Loads for Buildings and Other Structures*. American Society of Civil Engineers: New York.

FEMA. 1997. *NEHRP Commentary on the Guidelines for the Seismic Rehabilitation of Buildings, FEMA 274*. Federal Emergency Management Agency: Washington, DC.

FEMA. 2000. *Prestandard and Commentary for the Seismic Rehabilitation of Buildings, FEMA-356*. Federal Emergency Management Agency: Washington, DC.

GSA. 2003. *Progressive Collapse Analysis and Design Guidelines for New Federal Office Buildings and Major Modernization Projects*. The U.S. General Services Administration.

Kim J, Hong S. 2011. Progressive collapse performance of irregular buildings. *The Structural Design of Tall and Special Buildings* **20**(6): 721–734.

Kim J, Lee Y. 2010. Seismic Performance Evaluation of Diagrid System Buildings. *The Structural Design of Tall and Special Buildings* **19**(7): 761–777.

MIDAS GenW. 2007. *General Structure Design System for Windows*. MIDAS Information Technology Co Ltd: Seoul, Korea.

Moon K, Connor JJ, Fernandez JE. 2007. Diagrid structural systems for tall buildings: characteristics and methodology for preliminary design. *The Structural Design of Tall and Special Buildings* **16**(2).

Moon KS. 2007. Diagrid Sturctural systems for tall buildings, characteristics and methodology for preliminary design. *The Structural Design of Tall and Special Buildings* **16**: 205–230.

Park S, Elnimeiri M, Sharpe DC, Krawczyk RJ. 2004. Tall building form generation by parametric design process. CTBUH Conference, Seoul, Korea.

SAP 2000. 2004. *Structural Analysis Program*. Computers and Structures: Berkeley.

Shi Y, Li ZX, Hao H. 2010. Methods for progressive collapse analysis of building structures under blast and impact loads. *Engineering Structures* **32**(6): 1691–1703.

Vollers K. 2008. Morphological scheme of second-generation non-orthogonal high-rises, CTBUH 8th World Congress.

AUTHORS' BIOGRAPHIES

Jinkoo Kim received his BS degree from Seoul National University, Korea. He received his MS and PhD degrees from the Department of Civil and Environmental Engineering, Massachusetts Institute of Technology. His research interests include performance evaluation and retrofit of building structures against earthquake loads and progressive collapse.

Jieun Kong received her BS degree from Sungkyunkwan University, Korea. Currently, she is a graduate student in the same university.

DOI: 10.1002/tal